Analytical theory of extraordinary optical transmission through realistic metallic screens

V. Delgado[1*], R. Marqués[1], and L. Jelinek[2]

[1]*Departamento de Electrónica y Electromagnetismo. Universidad de Sevilla Avenida de Reina Mercedes, 41012, Sevilla*

[2]*Department of Electromagnetic Field. Czech Technical University in Prague 166 27, Prague, Czech Republic*

[*]*Corresponding author: vdelgado@us.es*

Abstract: An analytical theory of extraordinary optical transmission (EOT) through realistic metallic screens perforated by a periodic array of subwavelength holes is presented. The theory is based on our previous work on EOT through perfect conducting screens and on the surface impedance concept. The proposed theory is valid for the complete frequency range where EOT has been reported, including microwaves and optics. A reasonably good agreement with electromagnetic simulations is shown in all this frequency range. We feel that the proposed theory may help to clarify the physics underlying EOT and serve as a first step to more accurate analysis.

OCIS codes: (050.0050) Diffraction and gratings; (050.1960) Diffraction theory.

References and links

1. T. W. Ebbesen, H. J. Lezec, H. F. Ghaemi, T. Thio, and P. A. Wolff, "Extraordinary optical transmission through sub-wavelength hole arrays," Nature (London) **391,** 667–669 (1998).
2. H. F. Ghaemi, T. Thio, D. E. Grupp, T. W. Ebbesen, and H. J. Lezec, "Surface plasmons enhance optical transmission through subwavelength holes," Phys. Rev. B **58**(15), 6779–6782 (1998).
3. M. Sarrazin, and J-P. Vigneron, "Optical properties of tungsten thin films perforated with a bidimensional array of subwavelength holes," Phys. Rev. E **68**, 016603 (2003)
4. M. Beruete, M. Sorolla, I. Campillo, J. S. Dolado, L. Martín-Moreno, J. Bravo-Abad, and F. J. García-Vidal, "Enhanced millimeter-wave transmission through subwavelength hole arrays," Opt. Lett. **29**(21), 2500–2502 (2004).
5. M. Sarrazin, and J-P. Vigneron, "Light transmission assisted by Brewster-Zennek modes in chromium films carrying a subwavelength hole array," Phys. Rev. B **71**, 075404 (2005)
6. R. F. Collin *Field Theory of Guided Waves*, Edt. IEEE Press, New York (1991), 2nd Ed.
7. J. B. Pendry, L. Martín-Moreno, and F. J. García-Vidal, "Mimicking surface plasmons with structured surfaces," Science **305,** 847–848 (2004).
8. M. M. J. Treacy, "Dynamical diffraction explanation of the anomalous transmission of light through metallic gratings," Phys. Rev. B **66**, 195105 (2002)
9. F. J. Garía de Abajo, R. Gómez-Medina, and J. J. Sáenz, "Full transmission through perfect conductor subwavelength hole arrays," Phys. Rev. E **72**, 016608 (2005)
10. C. C. Chen, "Transmission of Microwave Through Perforated Flat Plates of Finite Thickness," IEEE Trans. Microwave Theory Tech. **21**(1), 1–6 (1973).
11. F. Medina, F. Mesa, and R. Marqués, "Extraordinary transmission through arrays of electrically small holes from a circuit theory perspective," IEEE Trans. Microwave Theory Tech. **56,** 3108–3120 (2008).
12. F. Medina,J. A. Ruiz-Cruz, F. Mesa, M. Rebollar, J. R. Montejo-Garai, and R. Marqués "Experimental verification of extraordinary transmission without surface plasmons," Appl. Phys. Lett. **95**, 071102 (2009).

#122150 - $15.00 USD Received 4 Jan 2010; revised 10 Feb 2010; accepted 22 Feb 2010; published 15 Mar 2010

13. R. Marqués, F. Mesa, L. Jelinek, and F. Medina, "Analytical theory of extraordinary transmission through metallic diffraction screens perforated by small holes," Opt. Express , **17**(7), 5571–5579 (2009).
14. Sergei Tretyakov, *Analytical Modeling in Applied Electromagnetics*, Edt. Artech House (2003).
15. R. Gordon, "Bethe's aperture theory for arrays," Phys. Rev. A **76**, 053806, (2007).
16. E. A. Coronado and G. C. Schatz, "Surface plasmon broadening for arbitrary shape nanoparticles: A probability approach," J. Chem. Phys. **119**, 3926–3934 (2003).

1. Introduction

First theories about extraordinary optical transmission (EOT) through metallic screens perforated by a periodic array of metallic holes [1] claimed the key role of surface plasmons (SPs) in this physical effect [2]. However, the same effect was soon reported in some metals with positive real part of the permittivity [3], and in metallic screens operating at microwave frequencies [4], where the behavior of metals is closer to a perfect conductor than to a solid plasma. In both cases SPs can not exist at the air-metal interfaces. In the first case, Zenneck waves can still be excited at such interfaces, and therefore they can be invoked in order to explain extraordinary transmission using a similar theoretical framework [5]. The explanation of EOT through perfect conducting screens in the frame of SP theories was more difficult, because surface waves can not be excited at flat perfect conducting interfaces. However, surface waves on corrugated perfect conducting interfaces were well known since far [6], and these surface waves – renamed as *spoof plasmons* – come to the rescue of the SP point of view [7]. At this point, it became clear that EOT can be linked to any kind of surface waves supported by the interface between air and the diffraction screen, and the results of SP theories become almost indistinguishable of those obtained from standard diffraction theory [8], [9].

The interest on wave transmission through perforated metallic screens is not new and these structures have been analyzed since far by electrical engineers. In [10] thick perfectly conducting screens were rigourously analyzed using the integral equation method. More recently, an equivalent waveguide circuit model for EOT has been proposed [11]. This approach has the advantage of also explaining EOT in configurations where excitation of surface waves is obviously impossible [12]. Using this point of view, some of the authors have recently developed an approximate analytical theory of EOT through perfect conducting screens [13]. In this paper, we present the generalization of this last theory to realistic metallic screens. The reported theory is based on the equivalent waveguide model already developed in [11] and [13], and on the surface impedance concept (see, for instance, [14] among others). In the frame of the present approach, this last concept is used to model realistic metallic screens as a pair of coupled surface impedances, yielding a "point to point" relation between the electric and magnetic fields at each side of the screen. Using this approximation, we can analyze EOT through realistic metallic screens from microwave frequencies (where metals behave as imperfect conductors) to optical frequencies (where metals mainly behave as solid plasmas). Some numerical results coming from our theory are compared with electromagnetic simulations of EOT in realistic structures and a reasonably good agreement is reported. The scope and limits of the reported approximation are also discussed.

2. Analysis

For simplicity, we will consider a square matrix of square holes perforated in a metallic diffraction screen as it is shown in Fig. 1 (the extension to rectangular holes and periodicities is straightforward). Due to the symmetry of the structure and for an incident TEM wave with an y-polarized electric field, the problem is equivalent to a TEM waveguide with electric walls at $y = -a/2$, 0 and $a/2$; magnetic walls at $x = -a/2$, 0 and $a/2$ and a discontinuity in the region of the screen [13]. The scattered fields at both sides of the screen can be decomposed on

#122150 - $15.00 USD Received 4 Jan 2010; revised 10 Feb 2010; accepted 22 Feb 2010; published 15 Mar 2010

even TE and TM modes [13]. Therefore, just at both interfaces of the screen ($z = \pm t/2$) the electromagnetic field can be expanded into the Fourier series

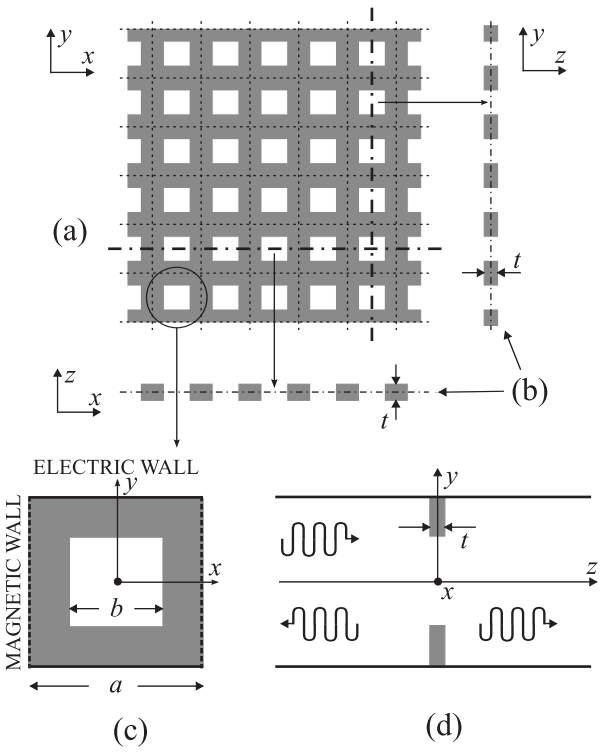

Fig. 1. Metallic screen perforated with square holes: front view (a) and two lateral cuts (b). Front (c) and lateral (d) views of the structure unit cell or equivalent waveguide. The screen has a finite thickness t.

$$E_y^- = 1 + R + \sum_{n=1,m=0}^{N,M} C^{\mathrm{TE}}_{nm,\mathrm{R}} f_{nm}(x,y) + \sum_{n=0,m=1}^{N,M} C^{\mathrm{TM}}_{nm,\mathrm{R}} f_{nm}(x,y) \tag{1}$$

$$E_y^+ = T + \sum_{n=1,m=0}^{N,M} C^{\mathrm{TE}}_{nm,\mathrm{T}} f_{nm}(x,y) + \sum_{n=0,m=1}^{N,M} C^{\mathrm{TM}}_{nm,\mathrm{T}} f_{nm}(x,y) \tag{2}$$

$$H_x^- = Y_0\,(1-R) - \sum_{n=1,m=0}^{N,M} Y^{\mathrm{TE}}_{2n,2m} C^{\mathrm{TE}}_{nm,\mathrm{R}} f_{nm}(x,y) - \sum_{n=0,m=1}^{N,M} Y^{\mathrm{TM}}_{2n,2m} C^{\mathrm{TM}}_{nm,\mathrm{R}} f_{nm}(x,y) \tag{3}$$

$$H_x^+ = Y_0 T + \sum_{n=1,m=0}^{N,M} Y^{\mathrm{TE}}_{2n,2m} C^{\mathrm{TE}}_{nm,\mathrm{T}} f_{nm}(x,y) + \sum_{n=0,m=1}^{N,M} Y^{\mathrm{TM}}_{2n,2m} C^{\mathrm{TM}}_{nm,\mathrm{T}} f_{nm}(x,y), \tag{4}$$

where $E_y^{\pm}$ and $H_x^{\pm}$ are the electric and magnetic fields at $z = \pm t/2$, T and R are the transmission and reflection coefficients, C^{TE} and C^{TM} are the amplitudes of the TE and TM modes excited in the screen, $f_{n,m}(x,y) = \cos(2n\pi x/a)\cos(2m\pi y/a)$, $Y_0 = -\sqrt{\varepsilon_0/\mu_0}$ is the admittance of free space and $Y^{\mathrm{TE}}_{2n,2m}$ and $Y^{\mathrm{TM}}_{2n,2m}$ are the TE and TM modal admittances of the equivalent waveguide:

$$Y^{\mathrm{TE}}_{2n,2m} = \frac{k^{nm}_{0z}}{k_0} Y_0 \quad \text{and} \quad Y^{\mathrm{TM}}_{2n,2m} = \frac{k_0}{k^{nm}_{0z}} Y_0, \tag{5}$$

#122150 - $15.00 USD Received 4 Jan 2010; revised 10 Feb 2010; accepted 22 Feb 2010; published 15 Mar 2010

where

$$k_{0,z}^{nm} = \sqrt{k_0^2 - \left(\frac{2n\pi}{a}\right)^2 - \left(\frac{2m\pi}{a}\right)^2} \tag{6}$$

is the propagation constant of the n,m mode (which are imaginary numbers below the first Wood's anomaly), and $k_0 = \omega\sqrt{\varepsilon_0\mu_0}$ is the vacuum wavenumber.

In the small hole approximation, the E_x^- and E_x^+ field components can be neglected due to the presence of additional virtual electric and magnetic walls at $y = 0$ and $x = 0$ respectively [13]. From standard waveguide theory, they are given by [6], [13]

$$E_x^- = \sum_{n,m=1}^{N,M} \left(\frac{m}{n} C_{nm,\mathrm{R}}^{\mathrm{TE}} - \frac{n}{m} C_{nm,\mathrm{R}}^{\mathrm{TM}}\right) g_{nm}(x,y) \approx 0 \tag{7}$$

$$E_x^+ = \sum_{n,m=1}^{N,M} \left(\frac{m}{n} C_{nm,\mathrm{T}}^{\mathrm{TE}} - \frac{n}{m} C_{nm,\mathrm{T}}^{\mathrm{TM}}\right) g_{nm}(x,y) \approx 0, \tag{8}$$

where $g_{n,m}(x,y) = \sin(2n\pi x/a)\sin(2m\pi y/a)$

Let us now consider the electromagnetic field inside the metallic screen. This is a well known problem that can be solved using the surface impedance concept (see e.g. [14]). For most metals, the propagation constant $k_\mathrm{s} = \omega\sqrt{\varepsilon\mu}$ is complex and very large from microwaves to optics. Assuming that it is still larger than all the transverse wavenumbers of all the meaningful Fourier modes in (1)–(4), $|k_\mathrm{s}| \gg 2n\pi/a$, the transverse dependence of the electromagnetic field inside the metal can be neglected with regard to its z dependence, and the differential equation for the electromagnetic field inside the metallic screen can be approximated by

$$\left\{\frac{\partial^2}{\partial z^2} + k_\mathrm{s}^2\right\} E_y \approx 0 \;\; ; \;\; \mathrm{i}\omega\mu H_x = -\frac{\partial E_y}{\partial z}. \tag{9}$$

This equation can now be easily solved giving a "point to point" linear relation between the electric and magnetic fields at both sides of the screen, which is independent of the specific dependence of these fields on x and y. After some straightforward calculations this relation is found as

$$\begin{pmatrix} E_y^+(x,y) + E_y^-(x,y) \\ E_y^+(x,y) - E_y^-(x,y) \end{pmatrix} \approx \begin{pmatrix} Z_{\mathrm{s},1} & 0 \\ 0 & Z_{\mathrm{s},2} \end{pmatrix} \begin{pmatrix} H_x^+(x,y) - H_x^-(x,y) \\ H_x^+(x,y) + H_x^-(x,y) \end{pmatrix} \tag{10}$$

with

$$Z_{\mathrm{s},1} = \frac{[1+\cos(k_\mathrm{s}t)]}{\mathrm{i}\sin(k_\mathrm{s}t)Y_\mathrm{s}} \;\text{ and }\; Z_{\mathrm{s},2} = \frac{\mathrm{i}\sin(k_\mathrm{s}t)}{[1+\cos(k_\mathrm{s}t)]Y_\mathrm{s}}, \tag{11}$$

where $Y_\mathrm{s} = (k_\mathrm{s}/k_0)Y_0$ is the wave admittance inside the metal and where $Z_{\mathrm{s},1}$ and $Z_{\mathrm{s},2}$ are commonly referred as "surface impedances" [14].

The next step in the analysis is to apply the small hole approximation[13], which in our case takes the form

$$\begin{aligned} &\int_{\mathrm{wg}} \left[\left(E_y^+ + E_y^-\right) - Z_{\mathrm{s},1}\left(H_x^+ - H_x^-\right)\right] f_{nm} dS = \int_{\mathrm{h}} \left[\left(E_y^+ + E_y^-\right) - Z_{\mathrm{s},1}\left(H_x^+ - H_x^-\right)\right] f_{nm} dS \\ &\approx \int_{\mathrm{h}} \left[\left(E_y^+ + E_y^-\right) - Z_{\mathrm{s},1}\left(H_x^+ - H_x^-\right)\right] dS = \int_{\mathrm{wg}} \left[\left(E_y^+ + E_y^-\right) - Z_{\mathrm{s},1}\left(H_x^+ - H_x^-\right)\right] dS \end{aligned} \tag{12}$$

#122150 - $15.00 USD Received 4 Jan 2010; revised 10 Feb 2010; accepted 22 Feb 2010; published 15 Mar 2010

$$\begin{aligned}&\int_{\mathrm{wg}}\left[\left(E_y^+-E_y^-\right)-Z_{\mathrm{s},2}\left(H_x^++H_x^-\right)\right]f_{nm}dS=\int_{\mathrm{h}}\left[\left(E_y^+-E_y^-\right)-Z_{\mathrm{s},2}\left(H_x^++H_x^-\right)\right]f_{nm}dS\\&\approx\int_{\mathrm{h}}\left[\left(E_y^+-E_y^-\right)-Z_{\mathrm{s},2}\left(H_x^++H_x^-\right)\right]dS=\int_{\mathrm{wg}}\left[\left(E_y^+-E_y^-\right)-Z_{\mathrm{s},2}\left(H_x^++H_x^-\right)\right]dS\end{aligned}\tag{13}$$

where subindex wg and h indicate integration in the waveguide and the hole cross sections, respectively. Taking into account the orthogonality properties of $f_{nm}(x,y)$ and after some straightforward calculations, we obtain

$$\begin{aligned}&(1-\delta_{n0})(1-Z_{\mathrm{s},1}Y^{\mathrm{TE}}_{2n,2m})C^{\mathrm{TE}}_{nm,\mathrm{T}}+(1-\delta_{n0})(1-Z_{\mathrm{s},1}Y^{\mathrm{TE}}_{2n,2m})C^{\mathrm{TE}}_{nm,\mathrm{R}}\\&+(1-\delta_{m0})(1-Z_{\mathrm{s},1}Y^{\mathrm{TM}}_{2n,2m})C^{\mathrm{TM}}_{nm,\mathrm{T}}+(1-\delta_{m0})(1-Z_{\mathrm{s},1}Y^{\mathrm{TM}}_{2n,2m})C^{\mathrm{TM}}_{nm,\mathrm{R}}\\&=2(2-\delta_{n0}-\delta_{m0})(1+R+T)+2(2-\delta_{n0}+\delta_{m0})Z_{\mathrm{s},1}Y_0(1-R-T)\end{aligned}\tag{14}$$

and

$$\begin{aligned}&(1-\delta_{n0})(1-Z_{\mathrm{s},2}Y^{\mathrm{TE}}_{2n,2m})C^{\mathrm{TE}}_{nm,\mathrm{T}}-(1-\delta_{n0})(1-Z_{\mathrm{s},2}Y^{\mathrm{TE}}_{2n,2m})C^{\mathrm{TE}}_{nm,\mathrm{R}}\\&+(1-\delta_{m0})(1-Z_{\mathrm{s},2}Y^{\mathrm{TM}}_{2n,2m})C^{\mathrm{TM}}_{nm,\mathrm{T}}-(1-\delta_{m0})(1-Z_{\mathrm{s},2}Y^{\mathrm{TM}}_{2n,2m})C^{\mathrm{TM}}_{nm,\mathrm{R}}\\&=2(2-\delta_{n0}-\delta_{m0})(-1-R+T)-2(2-\delta_{n0}-\delta_{m0})Z_{\mathrm{s},2}Y_0(1-R+T).\end{aligned}\tag{15}$$

where δ_{nm} is the Kronencker delta fucntion. The above expressions, altogether with

$$C^{\mathrm{TM}}_{nm,\mathrm{T}}\approx\frac{m^2}{n^2}C^{\mathrm{TE}}_{nm,\mathrm{T}}\ \text{ and }\ C^{\mathrm{TM}}_{nm,\mathrm{R}}\approx\frac{m^2}{n^2}C^{\mathrm{TE}}_{nm,\mathrm{R}}\tag{16}$$

which are obtained from (7) and (8), allow for the determination of the coefficients $C^{\mathrm{TE}}_{nm,\mathrm{R}}$, $C^{\mathrm{TM}}_{nm,\mathrm{R}}$, $C^{\mathrm{TE}}_{nm,\mathrm{T}}$, and $C^{\mathrm{TM}}_{nm,\mathrm{T}}$ as linear functions of the reflection and transmission coefficients R and T.

We still need two more equations in order to determine R and T. These equations are obtained applying the boundary conditions at both sides of the hole. It can be modeled as a hollow metallic waveguide with an evanescent dominant TE_{10} mode. As far as the hole can be considered small, we can neglect the effect of higher order modes and consider that only this dominant mode is excited in the hole. In this approximation, there is a relation similar to (10) between the electromagnetic fields at both sides of the hole with $Z_{\mathrm{s},1}$ and $Z_{\mathrm{s},2}$ replaced by the hole surface impedances

$$Z_{\mathrm{h},1}=\frac{[1+\cos(k_{\mathrm{h}}t)]}{\mathrm{i}\sin(k_{\mathrm{h}}t)Y_{\mathrm{h}}}\ \text{ and }\ Z_{\mathrm{h},2}=\frac{\mathrm{i}\sin(k_{\mathrm{h}}t)}{[1+\cos(k_{\mathrm{h}}t)]Y_{\mathrm{h}}},\tag{17}$$

where $k_{\mathrm{h}}=\sqrt{k_0^2-(\pi/b)^2}$ and $Y_{\mathrm{h}}=(k_{\mathrm{h}}/k_0)Y_0$ are the (imaginary) propagation constant and wave admittance of the aforementioned TE_{10} k mode. Therefore, the fields at both sides of the hole satisfy the following integral boundary conditions

$$\int_{\mathrm{h}}\left[\left(E_y^++E_y^-\right)-Z_{\mathrm{h},1}\left(H_x^+-H_x^-\right)\right]dS\approx0\tag{18}$$

$$\int_{\mathrm{h}}\left[\left(E_y^+-E_y^-\right)-Z_{\mathrm{h},2}\left(H_x^++H_x^-\right)\right]dS\approx0,\tag{19}$$

which yield

#122150 - $15.00 USD Received 4 Jan 2010; revised 10 Feb 2010; accepted 22 Feb 2010; published 15 Mar 2010

$$(1+T+R)+Z_{\mathrm{h},1}Y_0(1-T-R)+\left[\sum_{n=1,m=0}^{N,M} C^{\mathrm{TE}}_{nm,\mathrm{T}}+C^{\mathrm{TE}}_{nm,\mathrm{R}}-Z_{\mathrm{h},1}Y^{\mathrm{TE}}_{2n,2m}(C^{\mathrm{TE}}_{nm,\mathrm{T}}+C^{\mathrm{TE}}_{nm,\mathrm{R}})\right.$$
$$\left.+\sum_{n=0,m=1}^{N,M} C^{\mathrm{TM}}_{nm,\mathrm{T}}+C^{\mathrm{TM}}_{nm,\mathrm{R}}-Z_{\mathrm{h},1}Y^{\mathrm{TM}}_{2n,2m}(C^{\mathrm{TM}}_{nm,\mathrm{T}}+C^{\mathrm{TM}}_{nm,\mathrm{R}})\right]\mathrm{sinc}\left(\frac{n\pi b}{a}\right)\mathrm{sinc}\left(\frac{m\pi b}{a}\right)=0 \tag{20}$$

$$(-1+T-R)-Z_{\mathrm{h},2}Y_0(1+T-R)+\left[\sum_{n=1,m=0}^{N,M} C^{\mathrm{TE}}_{nm,\mathrm{T}}-C^{\mathrm{TE}}_{nm,\mathrm{R}}-Z_{\mathrm{h},2}Y^{\mathrm{TE}}_{2n,2m}(C^{\mathrm{TE}}_{nm,\mathrm{T}}-C^{\mathrm{TE}}_{nm,\mathrm{R}})\right.$$
$$\left.+\sum_{n=0,m=1}^{N,M} C^{\mathrm{TM}}_{nm,\mathrm{T}}-C^{\mathrm{TM}}_{nm,\mathrm{R}}-Z_{\mathrm{h},2}Y^{\mathrm{TM}}_{2n,2m}(C^{\mathrm{TM}}_{nm,\mathrm{T}}-C^{\mathrm{TM}}_{nm,\mathrm{R}})\right]\mathrm{sinc}\left(\frac{n\pi b}{a}\right)\mathrm{sinc}\left(\frac{m\pi b}{a}\right)=0 \tag{21}$$

with $\mathrm{sinc}(\theta)=\sin(\theta)/\theta$.

Equations (14)-(16) and (20)-(21) make the system of equations that determines the values of T and R, as well as the C_{nm} coefficients. In practical computations series must be truncated. As it is discussed in [13], this truncation can be safely made at $N,M=\mathrm{round}(a/b)$. The accuracy of the above formulas can be improved if the actual width of the hole b is replaced by an effective width $b_{\mathrm{eff}}=b+2\delta$, where δ is the skin depth of the metal. For lossy conductors δ can be evaluated as $\delta=\sqrt{2/(\omega\mu\sigma)}$, and for solid plasmas it can be evaluated as $\delta=\lambda_{\mathrm{p}}/(2\pi)$, where λ_{p} is the plasma wavelength.

The main approximation underlying our analysis is in Eqs. (12) and (13). This approximation was first suggested in [15] and assumes that the size of the hole is so small that the variation of the functions $f_{nm}(x,y)$ can be neglected through the hole (this approximation also implies that n and m can not be taken very large, and leads to the condition $N,M=\mathrm{round}(a/b)$ mentioned above). It is clear that the smaller the hole the better the approximation. Another key approximation is in Eqs. (7) and (8), which implies that E_x is neglected in the hole. This approximation is suggested by the specific geometry of the problem and it is confirmed by electromagnetic simulations (not shown). Both approximations were successfully applied in [13] for the analysis of EOT through perfect conducting metallic screens. The surface impedance approximation (9) - (11) can be only applied if the absolute value of the complex dielectric constant of the screen is much larger than that of the surrounding medium. This condition is usually fulfilled by most metals except at very high frequencies, in the ultraviolet range. Finally, we have considered only one mode in the hole in (18) - (19), which is justified if the hole is substantially smaller than the periodicity. All these approximations, taken altogether, results in the system of equations (14)-(16) and (20)-(21), whose coefficients are all analytical expressions, which can be run in a PC with an almost negligible computation time. For instance, the typical computation time for a frequency point in the plots shown below is less than 1μs using our model, whereas the typical computation time for a single frequency point using the commercial solver *CST Microwave Studio* is several min.

3. Numerical results

In Figs. 2 to 5 the transmission coefficient obtained from the reported theory and from electromagnetic simulations using *CST Microwave Studio* are plotted for frequencies ranging from GHz to optical, and employing different hole sizes, screen thicknesses and metals. In Figs. 2 and 3 the metals are modeled by finite conductivity σ

#122150 - $15.00 USD Received 4 Jan 2010; revised 10 Feb 2010; accepted 22 Feb 2010; published 15 Mar 2010

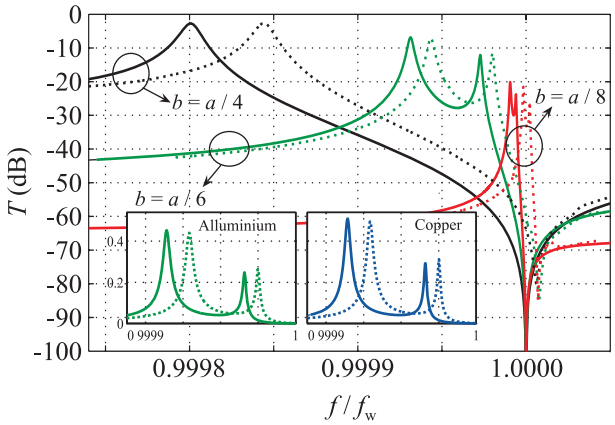

Fig. 2. Transmission coefficient in decibels versus normalized frequency (where $f_w = c/a$ is the Wood's anomaly frequency and c is the speed of light in vacuum) of the structure shown in Fig. 1 for $a = 30$ mm ($f_w \approx 10$ GHz), $t = a/10$ and different values of b. Solid lines correspond to the analytical model and dotted lines correspond to data from CST. In the main plot the metal is aluminium modeled by a finite conductivity ($\sigma = 37.8 \times 10^6$ S/m). In the inner plots the transmission of screens made of aluminium and copper ($\sigma = 59.6 \times 10^6$ S/m) with $b = a/6$ is compared.

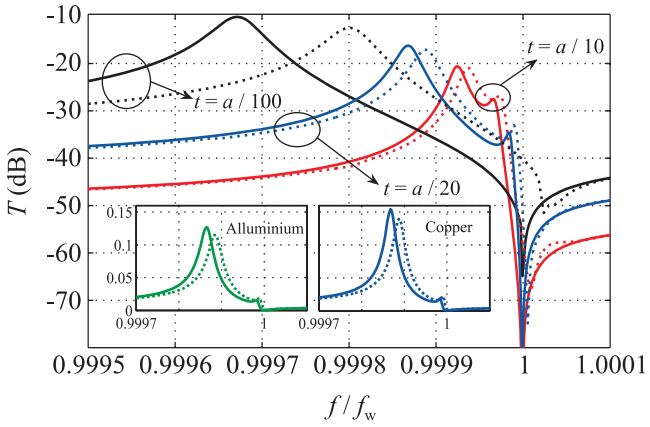

Fig. 3. Transmission coefficient in decibels versus normalized frequency for $a = 300$ μm ($f_w = c/a \approx 1$ THz), $b = a/6$ and different values of t. Solid lines correspond to the analytical model and dotted lines correspond to data from CST. In the main plot the metal is copper modeled by a finite conductivity ($\sigma = 59.6 \times 10^6$ S/m). In the inner plots the transmission of screens made of aluminium ($\sigma = 37.8 \times 10^6$ S/m) and copper with $t = a/20$ is compared.

#122150 - $15.00 USD Received 4 Jan 2010; revised 10 Feb 2010; accepted 22 Feb 2010; published 15 Mar 2010

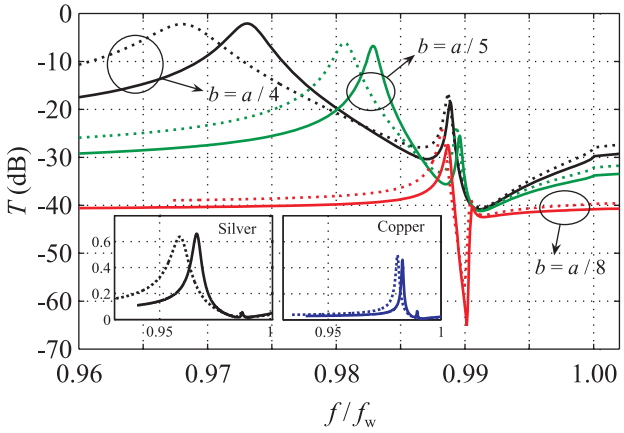

Fig. 4. Transmission coefficient in decibels versus normalized frequency for $a = 1$ μm ($f_w = c/a \approx 300$ THz), $t = a/10$ and different values of b. Solid lines correspond to the analytical model and dotted lines correspond to data from CST. In the main plot the metal is silver modeled by a Drude-Lorentz permittivity ($\omega_p = 2\pi \times 2175$ THz and $f_c = 2\pi \times 4.35$ THz). In the inner plots the transmission of screens made of silver and copper ($\omega_p = 2\pi \times 1914$ THz and $f_c = 2\pi \times 8.34$ THz) with $b = a/4$ is compared.

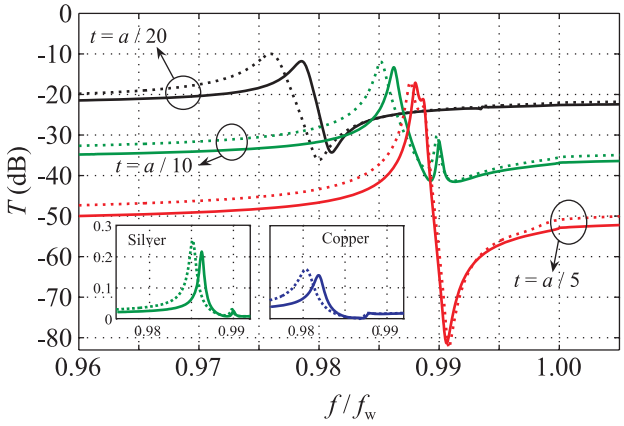

Fig. 5. Transmission coefficient in decibels versus normalized frequency for $a = 1$ μm ($f_w = c/a \approx 300$ THz), $b = a/6$ and different values of t. Solid lines correspond to the analytical model and dotted lines correspond to data from CST. In the main plot the metal is silver modeled by a Drude-Lorentz permittivity ($\omega_p = 2\pi \times 2175$ THz and $f_c = 2\pi \times 4.35$ THz). In the inner plots the transmission of screens made of silver and copper ($\omega_p = 2\pi \times 1914$ THz and $f_c = 2\pi \times 8.34$ THz) with $t = a/10$ is compared.

#122150 - $15.00 USD Received 4 Jan 2010; revised 10 Feb 2010; accepted 22 Feb 2010; published 15 Mar 2010

$$\varepsilon \approx \mathrm{i}\frac{\sigma}{\omega\varepsilon_0} \tag{22}$$

and in Figs. 4 and 5 by a Drude-Lorentz permittivity

$$\varepsilon \approx \varepsilon_0 \left(1 - \frac{\omega_\mathrm{p}^2}{\omega(\omega - \mathrm{i}\, f_\mathrm{c}')}\right), \tag{23}$$

where ω_p is the plasma frequency and f_c' is the collision frequency of electrons. For thin screens, with thicknesses of the order of the mean free path of the electrons or less, this frequency is affected by the collisions with the boundaries of the screen and differs from its value for bulk metals. Although the accurate determination of the corresponding correction to the electron frequency of collision is outside the scope of this paper, in order to make our results as realistic as possible, we introduced the correction proposed in [16], which for a plane metallic slab can be written as:

$$f_\mathrm{c}' = f_\mathrm{c}\left(1 + \frac{l_\mathrm{e}}{2t}\right) \tag{24}$$

here f_c is the collision frequency for bulk metals. Since the same correction was included in theoretical calculations and in electromagnetic simulations, the comparison of the results obtained from both approaches is not affected by this correction.

A very good qualitative agreement and reasonably good quantitative agreement in the position of the transmission peaks in relation to the Wood's anomaly frequency and their shape is found between theory and simulations (Figs. 2 to 5) for presented values of the screen thickness and hole size. The accuracy is higher for small holes (as we employ more modes in the Fourier expansion) and wider thickness (the hole is closer to a waveguide). This agrement is present for frequencies ranging from microwaves to optics, making apparent the wide range of application of the reported theory. A specific comment deserves the accurate prediction of the amplitude of the peaks by the theory, a fact that shows its usefulness for the quantitative analysis of losses in EOT through metallic screens.

At this point it may be worth to mention that, apart from the geometrical parameters such as periodicity a, hole size b and screen thickness t, the impedances $Z_{\mathrm{s},1}$, $Z_{\mathrm{s},2}$ (11) are the only parameters which characterize the structure in our theory. These impedances summarize all the constitutive electromagnetic properties of the screen, and determine its response regarding EOT. In the limit of perfectly conducting screens it is $1/Y_\mathrm{s} \to 0$ and $Z_{\mathrm{s},2} \to 0$, in which case (10) reduces to $E_y^+ = E_y^- = 0$ and the analysis reduces to that reported in [13], which can be considered as a particular case of the present theory.

4. Conclusion

Along this paper an analytical theory of EOT through realistic metallic screens perforated by a periodic array of subwavelength holes has been proposed. This theory is based on the equivalent waveguide model previously reported in [11] and [13], and on the surface impedance approach (10)-(11), which characterizes the material properties of the screen. The combination of both approaches allows for the development of an analytical theory valid for frequencies ranging from microwaves to optics, which includes the whole frequency range where EOT has been reported. Thus, the proposed theory provides an unifying approach to the phenomenon of EOT through metallic screens, identifying and clarifying the role of the most relevant physical parameters: periodicity, hole size and screen impedance. Apart from this theoretical interest, the good agreement between theory and electromagnetic simulations shows that the present

#122150 - $15.00 USD Received 4 Jan 2010; revised 10 Feb 2010; accepted 22 Feb 2010; published 15 Mar 2010

approach also provides a very efficient numerical tool for the analysis of EOT in realistic structures. It can be used directly or as a preliminary step before going to more sophisticated and time consuming numerical analysis.

Acknowledgments

This work has been supported by the Spanish Ministerio de Educación y Ciencia and European Union FEDER funds (TEC2007-68013-C02-01, and CSD2008-00066), and by Junta de Andalucía (project TIC–253). L. Jelinek also thanks for the support of the Czech Grant Agency (project no. 102/09/0314).

#122150 - $15.00 USD Received 4 Jan 2010; revised 10 Feb 2010; accepted 22 Feb 2010; published 15 Mar 2010